Heliyon 10 (2024) e24567

Contents lists available at ScienceDirect

Heliyon

journal homepage: www.cell.com/heliyon

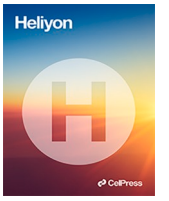

Research article

Hydroalcoholic extract from *Sechium edule* (Jacq.) S.w. root reverses oleic acid-induced steatosis and insulin resistance *in vitro*

Zimri Aziel Alvarado-Ojeda [a], Alejandro Zamilpa [b], Alejandro Costet-Mejia [b], Marisol Méndez-Martínez [c], Celeste Trejo-Moreno [a], Jesús Enrique Jiménez-Ferrer [b], Ana Maria Salazar-Martínez [d], Mario Ernesto Cruz-Muñoz [a], Gladis Fragoso [d,**], Gabriela Rosas-Salgado [a,*]

[a] *Facultad de Medicina, Universidad Autónoma Del Estado de Morelos, Leñeros S/N, Cuernavaca, Morelos, 62350, Mexico*
[b] *Laboratorio de Farmacología, Centro de Investigaciones Biomédicas Del Sur, Instituto Mexicano Del Seguro Social, Xochitepec, Morelos, 62790, Mexico*
[c] *Departamento de Sistemas Biológicos, Universidad Autónoma Metropolitana-Xochimilco, 04960, Mexico City, Mexico*
[d] *Instituto de Investigaciones Biomédicas, Universidad Nacional Autónoma de México, Coyoacán, 04510, Mexico City, Mexico*

ARTICLE INFO

Keywords:
Hepatocyte
Steatosis
Oleic acid
Sechium edule
Insulin resistance
Antioxidant/anti-inflammatory activity

ABSTRACT

Steatosis is characterized by fat accumulation and insulin resistance (IR) in hepatocytes, which triggers a pro-oxidant, pro-inflammatory environment that may eventually lead to cirrhosis or liver carcinoma. This work was aimed to assess the effect of *Sechium edule* root hydroalcoholic extract (rSe-HA) (rich in cinnamic and coumaric acid, among other phenolic compounds) on triglyceride esterification, lipid degradation, AMPK expression, and the phosphorylation of insulin receptor in a Ser^{312} residue, as well as on the redox status, malondialdehyde (MDA) production, and the production of proinflammatory cytokines in an *in vitro* model of steatosis induced by oleic acid, to help develop a phytomedicine that could reverse this pathology. rSe-HA reduced triglyceride levels in hepatocyte lysates, increased lipolysis by activating AMPK at Thr^{172}, and improved the redox status, as evidenced by the concentration of glycerol and formazan, respectively. It also prevented insulin resistance (IR), as measured by glucose consumption and the phosphorylation of the insulin receptor at Ser^{312}. It also prevented TNFα and IL6 production and decreased the levels of MDA and nitric oxide (ON). Our results indicate that rSe-HA reversed steatosis and controlled the proinflammatory and prooxidant environment in oleic acid-induced dysfunctional HepG2 hepatocytes, supporting its potential use to control this disorder.

1. Introduction

Metabolic dysfunction-associated fatty liver (MAFLD) is a spectrum of liver disorders, ranging from fat accumulation in the liver to

* Corresponding author. Facultad de Medicina, Universidad Autónoma del Estado de Morelos, 62350, Mexico.
** Corresponding author. Instituto de Investigaciones Biomédicas, UNAM, Mexico City, Mexico.
E-mail addresses: zimrihazi@gmail.com (Z. Aziel Alvarado-Ojeda), azamilpa_2000@yahoo.com.mx (A. Zamilpa), alejandro.costet@gmail.com (A. Costet-Mejia), mm.mary87@gmail.com (M. Méndez-Martínez), trejomc@hotmail.com (C. Trejo-Moreno), enriqueferrer_mx@yahoo.com (J.E. Jiménez-Ferrer), anamsm@biomedicas.unam.mx (A.M. Salazar-Martínez), mario.cruz@uaem.mx (M.E. Cruz-Muñoz), gladis@unam.mx (G. Fragoso), gabriela.rosas@uaem.mx (G. Rosas-Salgado).

https://doi.org/10.1016/j.heliyon.2024.e24567
Received 29 August 2023; Received in revised form 17 December 2023; Accepted 10 January 2024
Available online 17 January 2024

inflammation, fibrosis, necrosis, and simple steatosis to steatohepatitis. The prevalence of MAFLD in the general population in the world has been estimated at 35 % [1], but it could exceed 50 % in Mexico [2]. This explosive increase in MAFLD prevalence has been related to changes in dietary habits and a widespread sedentary lifestyle. Hepatic steatosis (HS) or fatty liver, a disease included in MAFLD, is a metabolic disorder characterized by the accumulation of fat in hepatocytes and insulin resistance (IR), which leads to a prooxidant, proinflammatory state that further aggravates metabolic syndrome, eventually resulting in serious diseases like nonalcoholic steatohepatitis (NASH), cirrhosis and, ultimately, liver cancer, a life-threatening condition [3,4]. Hepatic steatosis is common in type-2 diabetic patients, as it is diagnosed in 50–75 % of these subjects [5]. In addition to changes in lifestyle, drugs like statins [6] or metformin [7] have shown value in treating HS, as they promote lipolysis by activating AMPK kinase at the Thr^{172} residue. They also overcome IR by reversing phosphorylation at the Ser^{312} residue of the insulin receptor [6,7].

However, while efficient, these medications fail to alleviate some alterations that accompany the disease, and a polypharmacy is often required for their control. Given the multifactorial origin and complexity of MAFLD, in addition to the contribution of oxidative stress (OS) and proinflammatory cytokines like TNFα and IL6 in its progression [8], phytomedicines (being composed of multiple molecules with different therapeutic targets) could be useful for their control, as they can act as fat reducers, enhance lipolysis, decrease the accumulation of reactive oxygen species (ROS) and prevent the establishment of a proinflammatory environment [9]; these actions could allow us to replace the current polydrug approach [9]. *Sechium edule* (Jacq.) Sw. is a member of the Cucurbitaceae family native to Mexico (Cadena-Iñiguez, 2010). While there are no reports on its use in traditional medicine to treat liver diseases, other research groups have studied different parts of the plant for this purpose, with encouraging results (Firdous et al., 2012; Yang et al., 2015, Previously, we reported that the chronic administration of angiotensin II (ANGII) resulted in steatosis, hypertriglyceridemia, necrosis, inflammation, and fibrosis: the hallmark of NASH and these conditions was reversed by a hydroalcoholic extract of *S. edule* roots, rich in cinnamic acid, coumaric acid, ferulic acid, and some terpenes [10,11]. Those compounds have been reported to reduce triglyceride levels and overcome IR and OS, in addition to reducing the levels of proinflammatory cytokines [12–16].

This work was aimed to extend the phytochemical analysis of the rSe-HA and to analyze its mode of action in an *in vitro* model of MAFLD induced by oleic acid (OA)—the most abundant lipid in patients with metabolic syndrome (MS) [17]—over triglyceride esterification, lipid degradation, AMPK and IR phosphorylation, and the phosphorylation of the insulin receptor in a Ser residue, as well as on the redox status, MDA production, and the production of proinflammatory cytokines, to help develop a phytomedicine that could reverse this pathology. The anti-lipogenic drug metformin, often used as a reference in pharmacological studies [18], was included as a positive control.

2. Experimental

2.1. Plant material

Roots of *Sechium edule* (Jacq.) Sw. (60 kg) were collected in Cuautlapan, Veracruz, Mexico (18°47′00.5" N, 97°0′17.5" W, 1721 m above mean sea level) in February–March. All plant material was identified by Abigail Aguilar-Contreras (IMSS, Centro Médico Nacional, Mexico City). Voucher specimens were stored for future reference (IMSS-15549). Plant species were confirmed as *S. edule* and included in www.theplantlist.org [19]. Fresh roots were cut into small pieces and placed in the dark under a continuous air flow at 50 °C for 72 h to be dehydrated. The dried material (14.4 kg) was ground in a mill (Pulvex, Mexico City, Mexico) until 3–5 mm particles were obtained, and then it was extracted (8 kg) by maceration in 12 L of a 3:2 ethanol/H_2O mixture per 5 kg of plant material for 24 h. The supernatant was filtered and concentrated under vacuum to yield a semi-liquid extract; finally, 712 g of dry extract were obtained by freeze-drying.

2.2. HPLC-PDA analysis of cinnamic acid

An HPLC analytical method was developed using a Waters 2695 separation module (Waters Corporation, Milford, MA, USA). Secondary metabolites were detected with a Waters 996 photodiode array detector using the Empower Pro software (Waters). Chromatographic separation was performed in a Supelcosil LC-F column (4 mm × 250 mm, 5 μm, Sigma-Aldrich, Bellefonte, PA, USA). For chemical identification, 10 μL of rSe-HA (2 mg/mL) and standards of cinnamic and coumaric acids (100 mg/mL, Sigma Aldrich) were injected at a concentration of 0.1 g/mL in analytical grade methanol were filtered through a 0.45-μM membrane and injected into the column. The mobile phase consisted of a gradient system of 0.5 % trifluoroacetic acid aqueous solution (solvent A) – acetonitrile (solvent B), increasing as follows: 0–1 min, 0 % B; 2–3 min, 5 % B; 4–20 min, 30 % B; 21–23 min, 50 % B; 24–25 min, 80 % B; 26–27 min, 100 % B; 28–30 min, 0 % B. The flow rate was 0.9 mL/min. The detection wavelength was 280 nm. Cinnamic acid and coumaric acid were identified by comparing retention times (RT) and UV spectra with the commercial standards. While the retention time (RT) of cinnamic acid was 16.35 min (λ = 219, 280 nm), the RT for coumaric acid was 9.96 min min (λ = 219, 310 nm).

Cinnamic acid and coumaric acid in rSe-HA were quantified through a calibration curves built using concentrations of 1.562 μg/mL, 3.12 μg/mL, 6.25 μg/mL, 12.5 μg/mL, 25 μg/mL, 50 μg/mL, and 100 μg/mL of both polyphenolic compounds. Each sample was injected by triplicate into the HPLC equipment, and the chromatograms were recorded at 280 *n*m for cinnamic acid and at 310 nm for coumaric acid respectively. The peaks of interest (Retention time 10.03 and 16.46) were integrated, and the area under the curve was plotted as a linear equation (y = 1945.6x − 461.88 for cinnamic acid and y = 74519+490386). The concentration of cinnamic and coumaric acids was reported as mg per gram of extract.

2.3. GC-MS of non-polar compounds from hydroalcoholic extract

The complete extract was subjected to a column chromatographic process to identify the major terpenoids and sterols. The hydroalcoholic extract (14 g) was absorbed in normal phase silica (20 g, 70–230 mesh, Merck) and separated on a glass column packed with silica gel (140 g) using a gradient of *n*-hexane/ethyl acetate as mobile phase. A total of 54 samples of 150 mL were collected and dried by low-pressure distillation using a rota-evaporator system (Heidolph-Laborota 4000). The thin-layer chromatography of each mixture allowed us to group these samples according to their chemical composition. This process produced three principal fractions (C1F1, 0.112 g; C1F2, 0.271 g; C1F3, 0.148 g; C1F4, 0.254 g, and C1F5, 0.704 g) which were subjected to a gasses-mass chromatography analysis. Briefly, Agilent Technology 6890 plus Gas Chromatograph system, provided by a 5973 N mass spectrometer and a simple quadrupole analyzer, Electron Impact (IE) ionization mode at 70 eV was used for this chemical analysis. The samples were separated on an HP 5MS capillary column (25 m long, 0.2 mm inner diameter, with a film thickness of 0.3 μm). The oven temperature was set at 40 °C for 2 min, then programmed from 40 to 260 °C at 10 °C/min and held for 20 min at 260 °C. The mass detector conditions were as follows: interface temperature, 200 °C, and mass acquisition range, 20–550. The injector and detector temperatures were set at 250 and 280 °C, respectively. Identification of non-polar compounds was performed by comparing their mass spectra with the National Institute of Standards and Technology (NIST) 1.7 Library.

2.4. Hepatocyte culture and viability assay

HepG2 cells were seeded in 24-well plates (Nunc ImmunoPlate, MaxiSorp, Roskilde, Demark) for all assays, except for MTT and glucose uptake, which were performed in 96-well dishes (Nunc ImmunoPlate, MaxiSorp, Roskilde, Demark) and Western blot assays, for which cells were seeded in Petri dishes (Sigma, St. Louis, MO, USA). The cells were cultured in maintenance media (low-glucose Dulbecco's modified Eagle medium, DMEM) (ATCC 30–2002) supplemented with 10 % fetal bovine serum (Sigma), 1 % nonessential amino acids (Sigma, D1781), 1 % L-glutamine (Sigma, D1578), and 1 % penicillin-streptomycin (Sigma, D1881), at 37 °C, under 5 % CO_2 for 48 h. The cells were seeded in maintenance media at concentrations of 5×10^5 in 24-cell culture plates (500 μL per well), 5×10^3 cells in 24-cell culture plates (200 μL per well), or 3×10^6 in 60 × 15 mm cell culture petri dishes (3mL/dish), depending on the experiment (all from Falcon, USA). After 24 h of culture, either metformin (2 mM) (Jiang et al., 2014) (PreDialPlus, Silanes) or rSe-HA (at the EC_{50}), both resuspended in maintenance media, was added, and the OA stimulus was maintained (section 2.7). DMSO diluted in maintenance media (Sigma) (60 %) was used as a death control.

Cell viability was determined by the trypan blue assay (Sigma). After removing the culture medium, 200 μL per well of trypsin in 1X EDTA solution (0.05 % trypsin, 0.02 % EDTA) in Hanks' saline solution (Sigma) were added, and the plates were incubated at 37 °C under 5 % CO_2 for 5 min. To halt the trypsin reaction, 600 μL of supplemented low-glucose DMEM were added, and the cell suspension was centrifuged at 377×*g* at 4 °C for 7 min. The supernatant was discarded, and the cells were resuspended in complete medium and assessed for viability with 1:10 trypan blue by counting cells in a hemocytometer.

2.5. Quantification of hepatic ALT/GPT in culture media

The concentration of alanine aminotransferase (ALT/GPT) in culture medium is an indicator of hepatocyte death by necrosis [20]. ALT/GPT was measured in culture medium by the International Federation of Clinical Chemistry (IFCC) method, which is based on determining reaction rates, using a commercial ALT/GPT kit (QCA, Amposta, Tarragona, Spain), following the manufacturer's instructions. Briefly, 185 μL of reagent A were placed in flat-bottom 96-well plates, followed by 19 μL of culture medium. After incubating for approximately 1 min, 46 μL of reagent B was added. The absorbance was measured at 340 nm in an ELISA reader (Molecular Devices, San Jose, CA, USA) after 1, 2, and 3. ALT/GPT concentration was calculated with the following equations:

1) ABS1 min − ABS2 min = ABSa
2) ABS2 min − ABS3 min = ABSb
3) (ABSa – ABSb) × 2140 = U/dL (ALT/GPT)

Where:

ABS_1 min is the absorbance after 1 min of reaction; ABS_2 min is the absorbance after 2 min of reaction; ABS_3 min is the absorbance after 2 min of reaction; ABS_a is the early reaction rate; ABS_b is the late reaction rate; and 2140 is a proportionality factor to consider temperature and wavelength.

2.6. OA-induced steatosis

Once HepG2 cells reached 80 % confluence in 24- or 96-well culture plates, the cells were treated with 1 mM oleic acid-albumin (OA/BSA) (Sigma D1881) diluted in low-glucose DMEM media supplemented as described in Section 2.3, for 48 h [13,21].

2.7. EC_{50} calculation

rSe-HA EC_{50} and E_{max} were determined by measuring intracellular lipid concentrations by spectrophotometry after staining with Oil Red O (Sigma). The cells were exposed to a single concentration of OA/BSA (1 mM) and five concentrations of rSe-HA (0.1875,

0.375, 0.75, 1.5, and 3 μg/mL) obtained by serial dilution in maintenance media. Untreated cells and metformin-treated cells (2 mM diluted in maintenance media) were included as negative and positive controls, respectively. A concentration of 0.375 μg/mL was used to calculate EC_{50}, as this concentration reversed intracellular lipid accumulation to levels similar as those observed in non-stimulated cells. EC_{50} was determined by the method described above, except that the cells were previously cultured with five concentrations of OA/BSA (0.5, 1, 2, 4, and 8 mM) for 24 h and then treated with metformin, rSe-HA (0.375 μg/mL), or medium alone. EC_{50} for rSe-HA ($m = 0.52$, $b = 0.17$) and metformin ($m = 0.17$, $b = 1.07$) were calculated with the Michaelis-Menten equation; E_{max} values were graphically determined with the same equation.

2.8. Oil Red O staining

After 48 h of culture, hepatocytes were fixed with 10 % formalin-PBS for 60 min at room temperature (RT). The cells were washed with ice-cold PBS, and 60 % isopropanol was added and left to stand for 5 min to permeabilize cell membranes. Lipid droplets in cells were stained with Oil Red O (Sigma) for 30 min. Then, hepatocytes were washed with ice-cold PBS to remove the excess of dye and left to stand for 5 min at RT. Finally, the cells were washed with PBS, and 100 % isopropanol was added (to release stained fatty acids upon the rupture of the cell membrane) and left to stand for 5 min. The medium was collected and analyzed in a microplate reader (VERSAmax, Molecular Devices) at 510 nm.

2.9. Triglyceride quantification in hepatocyte lysates

After 48 h of culture, the cells were lysed in lysis buffer (50 mM Tris-HCl, 150 mM NaCl; 0.1 % Tritonx-100) (Sigma) at RT. Then, the plates were centrifuged at 2500 rpm for 5 min; the supernatants were collected, and triglyceride (TG) concentration was measured with the Triglycerides-LQ kit (QCA) (QCA, Amposta, Tarragona, Spain), following the manufacturer's instructions. Briefly, 5 μL of cell lysate were added to 96-well plates. Then, 200 μL of color reagent included in the kit was added, incubated for 5 min at RT, and read at 510 nm in an ELISA reader (VERSAmax). TG concentration was calculated with the following formula: $\Delta_{Problem}/\Delta_{Standard} \times 200$ mg/dL = mg/dL TG.

2.10. Glycerol quantification in culture medium

Glycerol was quantified in culture medium with the Colorimetric Assay Glycerol Kit (Sigma, MAK117) [22]. Briefly, 10 μL of culture medium for each treatment were transferred to 96-well plates and 100 μL/well of the Master Reaction Mix was added; the plates were incubated for 20 min at RT, in the dark. Then, absorbance was measured at 570 nm. A standard curve was built, and the following equation was used to calculate glycerol concentrations: $C = (A_{570})$ sample/slope.

2.11. Reducing power by MTT

Reducing power assessment is based on the formation of formazan from 3-(4,5-dimethylthiazol-2-yl)-2,5-diphenyltetrazole (MTT) bromide by succinate dehydrogenase or other reductive enzymes [23,24]. After a 24-h treatment, the medium was discarded, and the cells were incubated with 20 μL of 5 mg/mL MTT (Sigma) solution at 37 °C for 4 h. After incubation, 100 μL of 10 % SDS-HCl 0.01 N (1:1) were added to each well, and the plates were incubated for 2 h at 37 °C. Absorbance was measured at 570 nm in a VERSAmax microplate reader.

2.12. Glucose uptake

2-DG consumption was measured by a colorimetric assay using the Uptake 2-DG kit (Sigma, MAK083), as previously reported [22]. Briefly, after 48 h of culture, the medium was removed and the cells were incubated for 40 min in 2 % BSA in KRPH buffer (20 mM HEPES, 5 mM KH_2PO_4, 1 mM $MgSO_4$, 1 mM $CaCl_2$, 136 mM NaCl and 4.7 mM KCl) (Sigma). Then, the cells were stimulated with 1 μM insulin for 20 min. Then, 10 mM 2-DG in KRPH medium was added and incubated for another 20 min. Upon medium removal, the cells were lysed in freeze-thaw cycles with reaction solution A (assay buffer plus enzyme mixture in an 8:2 ratio). Then, the plates were incubated at 37 °C for 60 min in the dark, and an extraction buffer was added and left to stand for 5 min. The reaction was stopped by reaction solution B (53 % glutathione reductase, 42 % DTNB substrate, and 5 % recycle mixture). Absorbance was readded at 412 nm, and 2-DG concentration was calculated from a standard curve.

2.13. Malondialdehyde (MDA) quantification

A 650-μL aliquot of culture medium was placed in an Eppendorf tube and added with 150 μL of 1-methyl-2-phenylindole (10 mM) (Sigma) and allowed to react with MDA to produce stable chromophores. The tubes were vortexed and added with 30 μL of HCL (37 %), shaken again, and incubated in the dark at 45 °C for 60 min to drive the reaction to completion. After incubation, the tubes were centrifuged at 300 × *g* for 15 min. Finally, the absorbance of the upper organic layer was measured in a plate reader at 586 nm. A standard curve of 4, 3, 2, 1, 0.5, 0.25 and 0.125 mM tetramethoxypropane (TMOP) (Sigma) was built. The result was expressed as μg/mg protein by the Bradford standard method (Sigma, B6916).

2.14. Nitrite quantification by the griess method

NO levels were measured as nitrite/nitrate (final products of NO metabolism) by the Griess reaction [25]. A 100 μL-aliquot of the medium was placed in 96-well plates and incubated with 100 μL of Griess reagent (0.1 % (1-naphthyl)-ethylenediamine and 1 % sulfanilamide in 2.5 % phosphoric acid) (Sigma) for 30 min at RT. Absorbance was measured at 540 nm in a VERSAmax microplate reader. The amount of NO in each sample was determined by a sodium nitrite standard curve.

2.15. IL6 and TNF-α quantification by sandwich ELISA

IL6 and TNFα were quantified by sandwich ELISA using commercial kits (ELISA MAX 430502, Biolegend, and BD OptEIA 555212, respectively), following the manufacturer's instructions. Briefly, 96-well, flat-bottom ELISA plates (Nunc ImmunoPlate) were coated with the respective capture antibody and incubated overnight at 4 °C in carbonate buffer (pH 9.6). Non-specific binding sites were blocked by incubating for 30 min at RT with PBS-1% albumin. Culture medium was added and incubated for 2 h at RT. The plates were then incubated with the corresponding horseradish peroxidase (HRP)-conjugated anti-cytokine detection antibody for 30 min at RT. Bound complexes were detected by reaction with tetramethylbenzidine (TMB) (Invitrogen, Carlsbad, CA, USA) after 30 min incubation in the dark. The reaction was stopped with 2 N H_2SO_4, and absorbance was measured at 450 nm at 37 °C on a VERSAmax ELISA plate reader. Standard curves were built to calculate the concentration of each cytokine. Concentrations were expressed as pg/mg protein

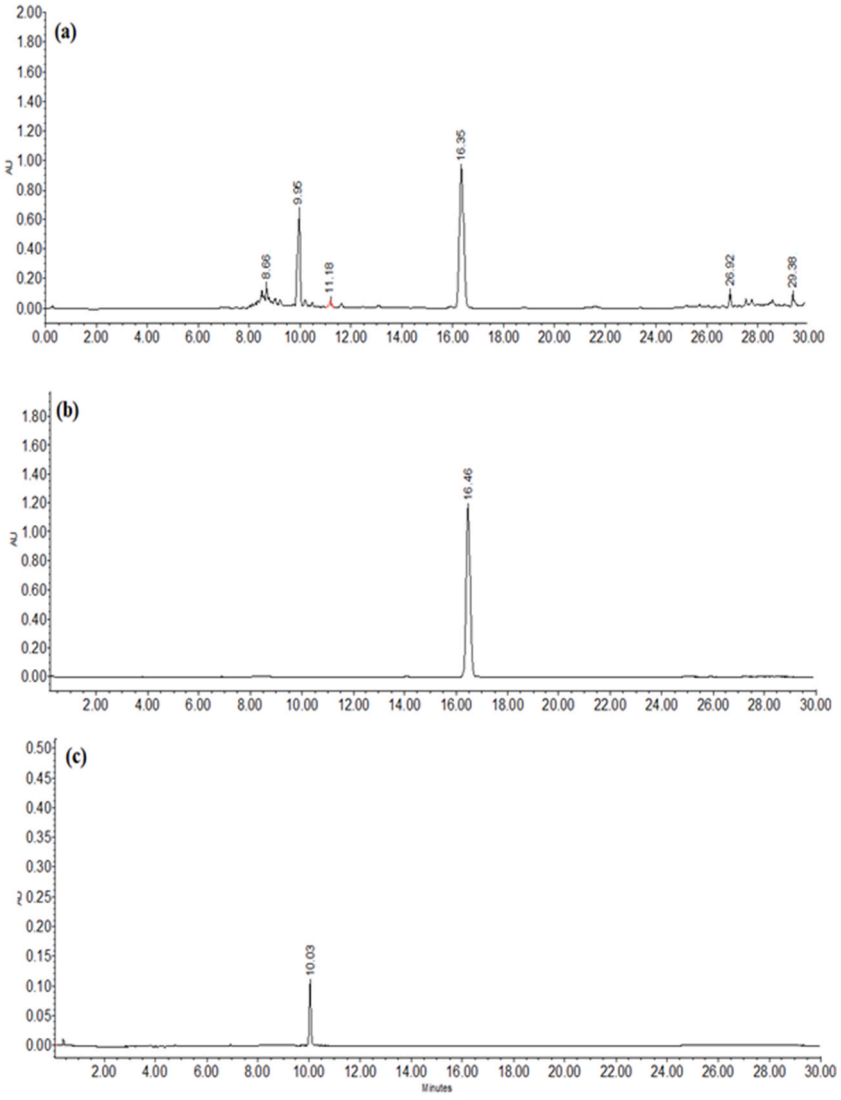

Fig. 1. CHROMATOGRAPHIC CHARACTERIZATION OF CINNAMIC AND COUMARIC ACIDS. Fingerprint of (a) hydroalcoholic extract at λ = 278 *n*m, (b) cinnamic acid at λ = 278 *n*m and (c) and coumaric acid at λ = 310 nm.

employing the Bradford assay (Sigma, B6916).

2.16. SDS-PAGE and western blot

For protein extraction, SDS-PAGE, and Western blot assays, 3×10^6 HepG2 cells were cultured as described above. The cells were mechanically lysed with a lysis buffer (25 mM Tris-HCL, pH 7.4, 2 mM EDTA, 0.5 % Triton X-100, protein inhibitor cocktail EDTA-free (Roche)) and centrifuged at 18 000×*g* for 10 min at 4 °C. Then, 90 μL of the supernatant were denatured with β-mercaptoethanol (Sigma). The samples were electrophoretically resolved on 10 % polyacrylamide-SDS (Sigma). Thereafter, the proteins were transferred onto polyvinylidene difluoride membranes (Immobilon-P, PVDF, Millipore) and blocked with skimmed milk in blocking buffer containing 5 % m/w nonfat dry milk, 1x TBS 0.2 % Tween-20 at RT for 1 h under gentle shaking. The membranes were incubated with anti-AMPK (1:500), anti-p(Thr^{172})-AMPK (1:500), anti-IRS (1:500), anti-p(Ser^{312})-IRS (1:500), and anti-actin (1:1000) (Cell Signaling Technology) antibodies for 2 h at RT, followed by five washes with 1 M Tris-base pH 7.5, 0.5 M EDTA, 150 mM NaCl, 1 % Tween 20. Afterwards, the membranes were treated with a secondary antibody (anti-rabbit-HRP, 1:1000, Cell Signaling Technology) diluted in blocking buffer for 2 h at RT. Antibody binding was detected with a chemiluminescence kit (ELC, General Electric) and Kodak X-ray film. The relative phosphorylation of each protein was determined with the ImageJ software, using the actin signal for data normalization.

2.17. Statistical analysis

All data were captured in Excel (Microsoft Co, Redmond WA, USA). Data are reported as bar graphs. Groups or treatments were compared by one-way ANOVA with a Tukey-Kramer post-hoc test. Data were analyzed with GraphPad InStat v.3.06 (GraphPad, San Diego, CA, USA). Differences were considered as significant for $P \leq 0.05$. In all graphs, significant differences between treatments or groups are indicated with different letters. The same letter in different groups indicate that there are no significant differences between those groups.

3. Results

3.1. Cinnamic acid and coumaric acids content in rSe-HA

Cinnamic acid (CA) was identified in the hydroalcoholic extract of the roots of *S. edule,* and it seems to be its most abundant constituent. A standard curve ($R^2 = 1$) was built with different concentrations of a commercial CA standard. As shown in Fig. 1a, the CA standard showed a RT of 16.46 min in the chromatogram, in good agreement with the RT value of 16.35 in the major peak for rSe-HA (Fig. 1b). This result was further verified by comparing UV spectra of rSe-HA and the CA standard; both spectra showed maximum absorbance at a wavelength of 278.1 and 310 *n*m, respectively. CA concentration in rSe-HA was calculated as $y = 97600.5x + 29\,590$, yielding a value of 1350 ± 0.00 μg/g. For coumaric acid, a standard showed a RT of 10.03 min in the chromatogram (Fig. 1c), in good agreement with the RT value of 9.95 for rSe-HA (Fig. 1b). For this compound, a yielding of 980 μg/g was obtained according to the equation $y = 74519x+490386$.

3.2. Identification of non-polar compounds

Chemical analysis of the less polar composition by GC-MS identified Squalene, Stigmastadiene, Stigmasterol, 2H-pyran-2-one

Table 1
Non-polar phytocomponents identified in retention times (RT) of different fractions of the hydroalcoholic extract of rSe-HA by GC-MS.

Fraction	RT (min)	Name	Molecular weight (g/mol)	Molecular Formula
C1F1	18.68	Hexadecanoic acid methyl ester	270.450	$C_{17}H_{34}O$
C1F2	18.68			
C1F3	18.8			
C1F5	18.68			
C1F1	19.42	Hexadecanoic acid (Palmitic acid)	256.43	$C_{16}H_{32}O_2$
C1F1	24.5	Hexadecanoic-acid-2-hydroxy-1-(hydroxymethyl)-ethyl-ester	330.50	$C_{19}H_{38}O_4$
C1F2	24.3			
C1F3	24.5			
C1F5	24.3			
C1F1	29.2	Squalene	410.73	$C_{30}H_{50}$
C1F3	29.2			
C1F1	38.1	Stigmasta-3,5-dien-7-one	410.7	$C_{29}H_{46}O$
C1F3	38.1			
C1F4	36.1	Stigmasterol	412.7	$C_{29}H_{48}O$
C1F4	20.7	2H-pyran-2-one, tetrahydro-6-nonyl	226.35	$C_{14}H_{26}O_2$
C1F5				
C1F5	32.5	Stigmastadiene	396.7	$C_{29}H_{48}$

tetrahydro-6-nonyl, Hexadecanoic-acid-2-hydroxy-1- (hydroxymethyl)-ethyl-ester, Hexadecanoic acid, Hexadecanoic acid methyl ester, Tetradecanoic acid, methyl ester among other fatty acids (Table 1). Chromatograms of these fractions are shown in Supplementary Fig. 1.

3.3. rSe-HA EC_{50} determination

The effect of different concentrations of rSe-HA was evaluated on HepG2 hepatocytes. Cell viability was assessed by trypan blue staining; in parallel, ALT/GPT was quantified in culture medium as an indicator of hepatocyte necrosis [20]. As shown in Supplementary Fig. 2 (A and B), none of the treatments modified cell viability after 24 h of culture, except for DMSO (death control). As shown in panel a, the count of viable cells showed a 5-fold increase ($P < 0.001$) with respect to time 0 in all treatments, whereas the count of DMSO-treated cells decreased by 46.5 %, a finding suggestive of hepatocyte necrosis (Supplementary Fig. 1 B). No significant differences were observed between any treatment with respect to untreated cells except for DMSO ($P < 0.001$).

To determine the EC_{50} of rSe-HA, HepG2 hepatocytes were cultured with 1 mM OA for 24 h and then treated with five different concentrations of the extract, under a continued OA stimulus for further 24 h. Absorbance due to lipid accumulation after 24 h of exposure to OA was 1.4; this value increased to 2.4 after 48 h of exposure to OA (an increase of 187.9 %) (Fig. 2 A). As shown, untreated cells did not exhibit lipid accumulation. Both rSe-HA (0.37 μg/mL) and metformin led to a significant decrease in this parameter ($P < 0.001$), restoring it to the level of non-stimulated cells, a value 47.64 % less with respect to OA-treated cells at 24 h. Meanwhile, rSe-HA at a concentration of 0.18 μg/mL decreased lipid accumulation by 290.6 % ($P < 0.001$); a concentration of 0.75 μg/mL showed a slight decrease (6.6 %, $P < 0.001$), and concentrations of 1.5 and 3 μg/mL failed to show any effect, since absorbance values were similar to those observed after 24 h of exposure to OA (Fig. 2 A). A concentration of 0.375 μg/mL was used for EC_{50} calculation, as this concentration reversed intracellular lipid accumulation to levels similar as those observed in non-stimulated cells.

To determine EC_{50}, a solution containing 0.375 μg/mL of the extract was challenged with different concentrations of OA (Fig. 2 B). rSe-HA EC_{50} was calculated as 0.20 μg/mL (equivalent to 0.27 ng of CA) while metformin EC_{50} was 0.8 μg/mL. E_{max} values were calculated as 0.7, 1.4, and 3.3 μg/mL for rSe-HA, metformin, and OA, respectively.

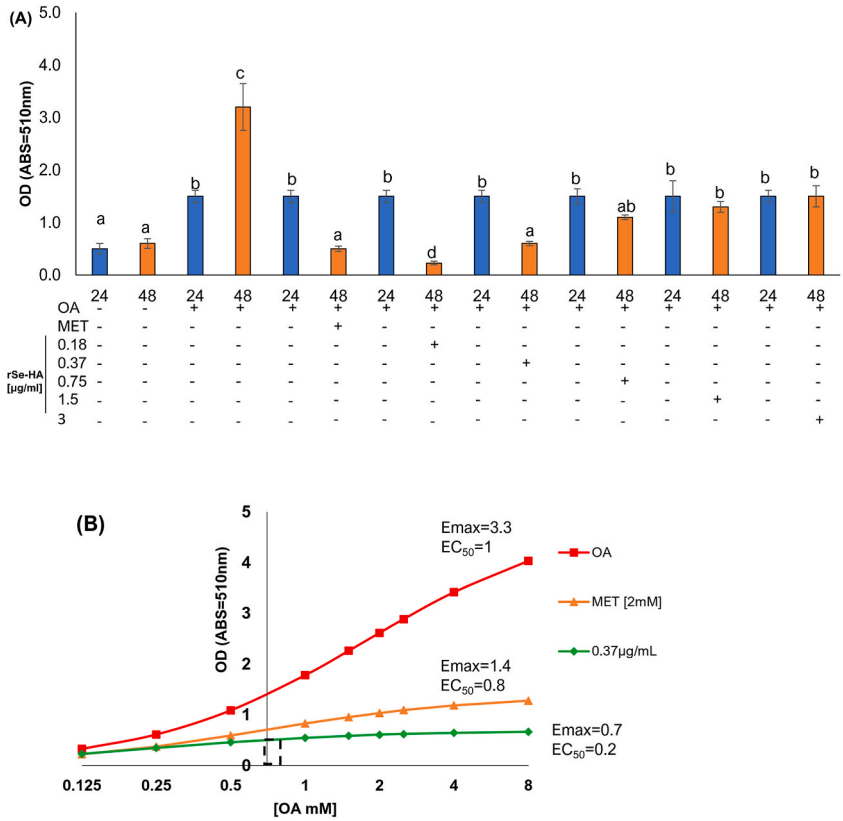

Fig. 2. EC_{50} CALCULATION. **(A)** Absorbance due to lipid accumulation by Oil Red O staining in HepG2 cells treated for 24 h with OA to induce steatosis, and for further 24 h with OA plus 2 mM metformin or 0.18, 0.37, 0.75, 1.5, or 3 μg/mL rSe-HA. The highest decrease in lipid accumulation was observed at a concentration of 0.37 μg/mL **(B)** HepG2 cells were treated with metformin (2 mM) or rSe-HA (0.37 μg/mL) and different OA concentrations (0.5, 1, 2, 4, 8 mM). rSe-HA EC_{50} was calculated as 0.20 μg/mL. Data are reported as mean ± SD. Differences between groups were determined by ANOVA and post hoc Tukey-Kramer test. The same letter in treatments or groups indicate that there are no significant differences between them; different letters in treatments indicate significant differences at $P < 0.05$. ABS = absorbance due to lipid accumulation at 510 nm.

3.4. rSe-HA reverses steatosis by increasing lipolysis

Lipolysis is a metabolic event by which fatty acids are degraded to produce energy. Normally, the cell activates this process in response to an energy demand; however, some drugs aiming to reduce intracellular lipid levels also trigger this process [3,4]. To determine whether the decrease in TG concentration by rSe-HA was due to a degradation of TG synthetized in the cells during OA exposure, two parameters were measured: glycerol concentration in the medium and the reducing status due to the activity of mitochondria or smooth endoplasmic reticulum during lipid degradation. This latter condition was observed as an increased rate of conversion of MTT to formazan [23,24]. Finally, it was assessed whether rSe-HA acts on AMPK kinase as metformin does.

The effect of rSe-HA on the concentration of esterified TG was evaluated at a dose of 0.20 μg/mL. HepG2 cells were either cultured without any treatment or with OA for 24 h to induce steatosis, and they were either maintained under these conditions for further 24 h or cultured for 24 h with OA plus metformin or rSe-HA for further 24 h, to reverse steatosis. As shown in Fig. 3 A, no significant changes in TG concentrations were observed between 24 and 48 h of culture in untreated cells. In cells treated with OA only, TG concentrations increased by 124.7 % ($P < 0.001$) after 24 h of culture with respect to untreated cells; this increase persisted at 48 h of culture. On the other hand, TG concentration in cells cultured with metformin or rSe-HA decreased by about 98 % and 99 % ($P < 0.001$), respectively, with respect to the levels observed at 24 h, bringing TG concentrations to values comparable with those in untreated cells.

As shown in Fig. 3 B, glycerol levels did not change in untreated cells at 24 or 48 h. Meanwhile, those levels were increased by 80 % in cells treated with OA at 24 h with respect to untreated control cells at 24 h ($P < 0.001$). On the other hand, while glycerol levels in OA-treated cells were decreased by 79 % ($P < 0.001$) at 48 h with respect to 24 h, they were increased by 81 % and 85 % ($P < 0.001$) in cells treated with metformin or rSe-HA, respectively. As shown in Fig. 3C, whilst no differences were observed in absorbance values due to formazan production in untreated cells at 24 and 48 h, absorbance values decreased by 83 % at 24 h in OA-treated cells with respect to control cells at the same time ($P < 0.001$). At 48 h, absorbance values decreased by 89 % in OA-treated cells ($P < 0.001$), but they were increased by 70 % and 80 % in metformin and rSe-HA-treated, respectively ($P < 0.001$). To investigate the mechanism of action of the extract to activate lipolysis, the relative amount of AMPK kinase and the one phosphorylated at Thr^{172} was studied at 48 h. As shown in Fig. 3 D–F, oleic acid significantly increased AMPK production with respect to untreated cells ($P < 0.001$). This effect was not modified by either metformin or rSe-HA (Fig. 3 D and E). However, both metformin and the extract significantly increased the levels of Thr^{172}-phosphorylated AMPK, with the extract being even more effective than metformin, as shown in Fig. 3 D and F ($P < 0.001$).

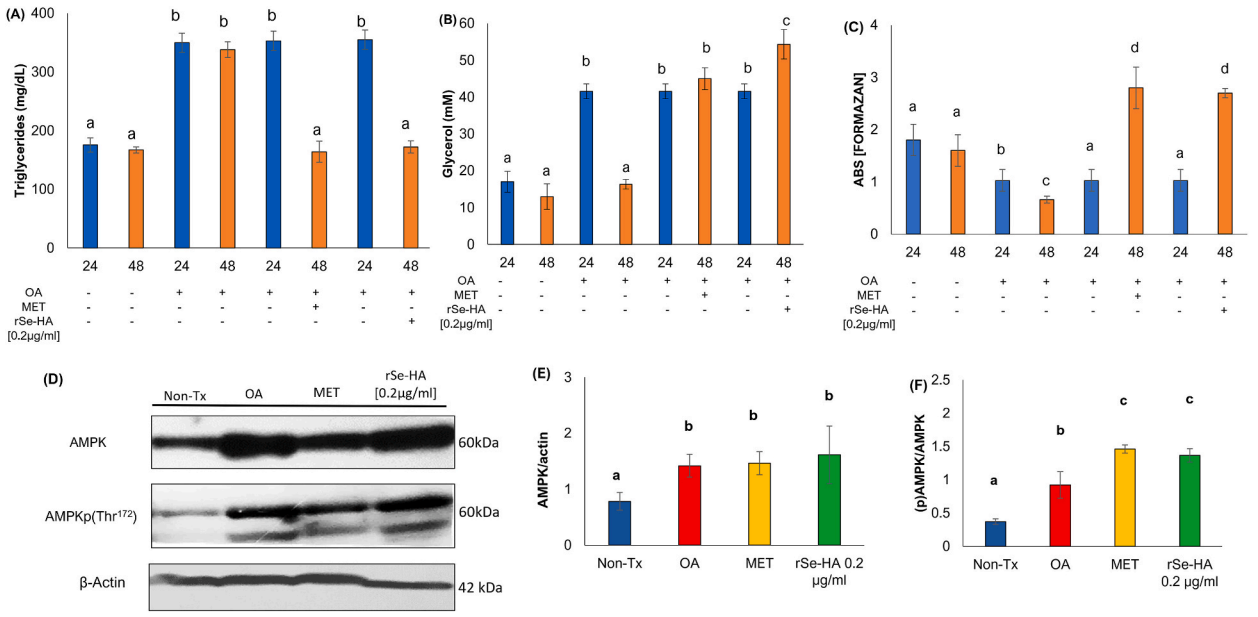

Fig. 3. rSe-HA ACTIVATES LIPOLYSIS BY ACTIVATING AMPK in Thr^{172} in HepG2. **(A)** Triglyceride (TG) concentration was determined in cell lysates. (**B**) Glycerol concentration was determined in medium culture; (**C**) Absorbance due to formazan produced from MTT reduction. Panels A, B, C show, on one hand, treatments compared with an untreated, control group at 24 and 48 h and, on the other hand, the effect of rSe-HA and metformin on all groups at different times. Data are reported as mean ± SD. The same letter in treatments or groups indicate that there are no significant differences between them; different letters in treatments indicate significant differences at $P < 0.05$. (D–F) Western Blot, anti AMPK and AMPK phosphorylated in Thr^{172} of the HepG2 cells treated for 24 h with OA to induce steatosis, and further 24 h with OA plus either 2 mM metformin or 0.20 μg/mL rSe-HA. Data are reported as the Mean ± SE. Differences with respect to untreated cells were determined by ANOVA and a Tukey-Kramer post hoc test. Significant differences with respect to the untreated group ($P \leq 0.001$) are indicated by different letters. Triglyceride, glycerol, and formazan assays were performed in triplicate. Western blot assays for total- and *p*-AMPK were performed in duplicate.

3.5. rSe-HA reversed insulin resistance

Insulin resistance (IR) is characterized by an abrupt decrease in glucose consumption and phosphorylation in a Ser residue in the insulin receptor. To determine whether exposure to OA and lipid accumulation inside HepG2 cells is linked to the development of IR, the capacity of cells to consume glucose was evaluated by a colorimetric assay, and Ser phosphorylation in IR was assessed by Western blot. HepG2 hepatocytes were cultured as described above, but these assays were focused on IR. As shown in Fig. 4 A, no differences were observed in glucose consumption at 24 and 48 h of culture in control cells; on the other hand, glucose consumption was decreased by 50 % in cells treated with OA for 24 h with respect to untreated cells at the same time. At 48 h, no changes were observed in OA-treated cells, while glucose consumption increased by 65.8 % and 63.3 % in metformin and rSe-HA-treated cells, respectively ($P < 0.001$). As shown in panels B and C, OA treatment reduced significantly ($P < 0.01$) the total levels of insulin receptor substrate (IRS)/Actin with respect to healthy cells at 48 h, and it significantly increased the level of the relation of phosphorylation of the receptor at Ser^{312}/total IRS (Fig. 4 D). On the other hand, both metformin and rSe-HA reduced total IRS/Actin levels ($P < 0.001$) (Fig. 4C), and both treatments significantly reduced the level of Ser^{312}-phosphorylated IRS/total IRS ($P < 0.001$). These results indicate that both metformin and rSe-HA were able to offset the effect of OA, inducing higher levels of glucose consumption than those observed in untreated cells.

3.6. rSe-HA reverses pro-oxidative environment

Lipid accumulation induces an increase in lipolysis, which in turn triggers an overproduction of ROS [26], which induce a pro-oxidative environment. To determine whether the increase in lipolysis rates induced by rSe-HA promoted a pro-oxidative environment, malondialdehyde (MDA) and nitrite concentration (two molecules that are produced under pro-oxidative conditions) were quantified in cell culture medium of HepG2 hepatocytes cultured as described above. As shown in Fig. 5A, healthy cells showed low MDA concentrations at 24 and 48 h of culture, as expected. When the cells were treated with OA alone, MDA concentrations significantly increased at 24 h ($P < 0.001$), remaining at a similar level at 48 h. In contrast, metformin caused a discrete decrease in MDA levels, whereas rSe-HA succeeded in reducing MDA concentrations to levels similar to those of the healthy group. Nitrite concentrations (Fig. 5 B) followed the same pattern; thus, whilst nitrite concentrations increased in OA-treated cells for 24 h ($P < 0.001$), this

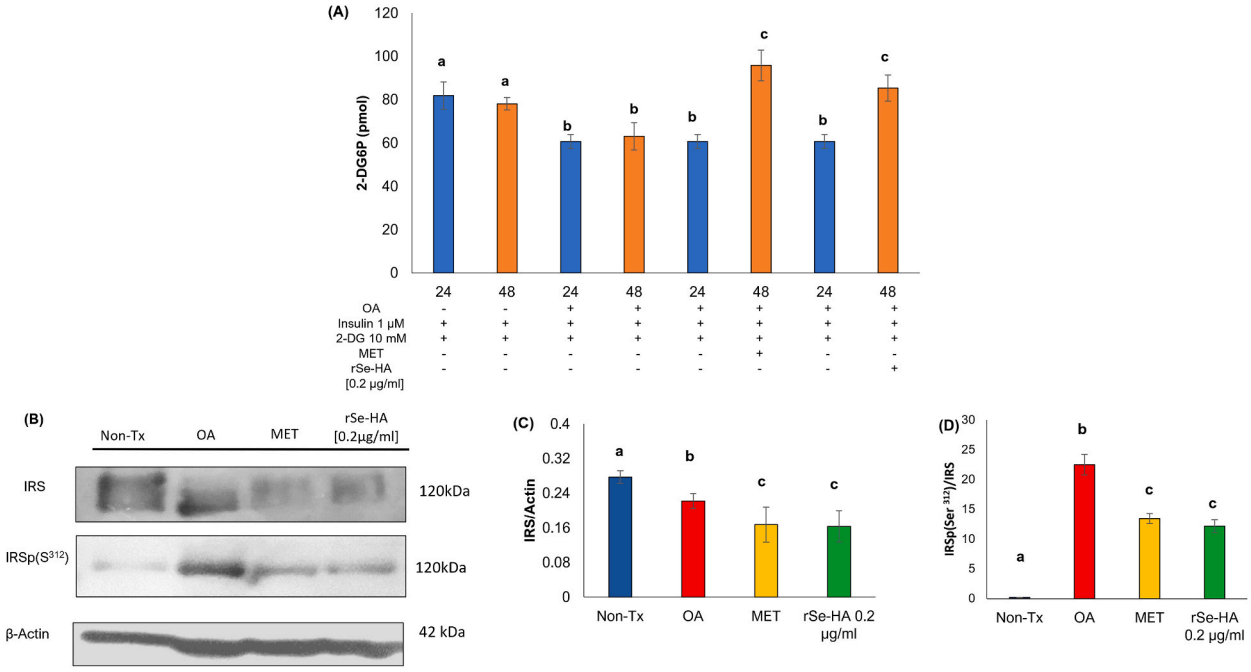

Fig. 4. rSe-HA REVERSES Ser^{312} PHOSPHORYLATION AND INCREASES GLUCOSE UPTAKE. HepG2 cells were treated for 24 h with 1 mM OA or maintenance medium (non-Tx) and with 1 mM OA plus 2 mM metformin or 0.20 µg/mL of rSe-HA for further 24 h. **(A)** In cells treated with OA, 2-DG6P concentration was reduced at 24 h, and these levels remained unchanged at 48 h, whereas treatment with metformin and rSe-HA reversed the low glucose consumption at 24 h, and both treatments even increased glucose consumption over that in untreated cells. **(B–D)** Western blot, anti-IRS phosphorylated in Ser^{312} in HepG2 cells treated for 24 h with OA to induce IR, and further 24 h with OA plus either 2 mM metformin or 0.20 µg/mL rSe-HA. Data are reported as mean ± SD. The same letter in treatments or groups indicate that there are no significant differences between them; different letters in treatments indicate significant differences at $P < 0.05$. Differences with respect to untreated cells were analyzed by ANOVA and a Tukey-Kramer post hoc test. Glucose uptake assays were performed in triplicate. Western blot assays for total- and Ser^{312}-p-IRS were performed in duplicate.

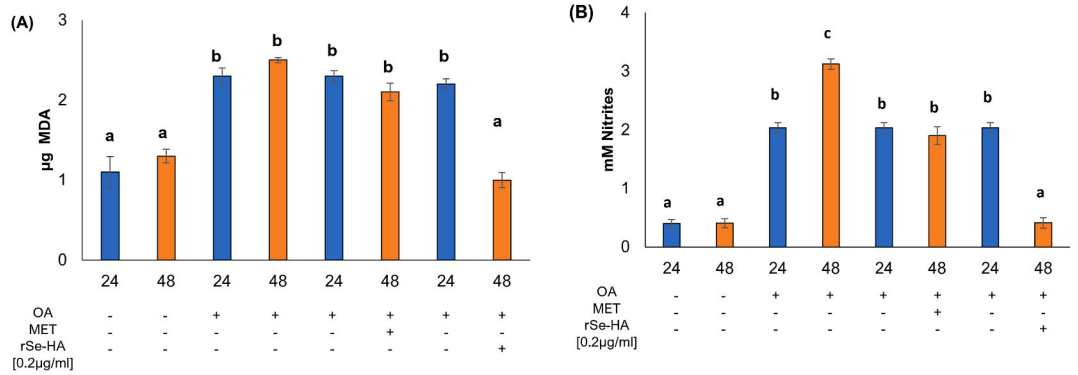

Fig. 5. MDA QUANTIFICATION. HepG2 cells were treated for 24 h with 1 mM OA or maintenance medium (non-Tx) and with 1 mM OA plus 2 mM metformin or 0.20 µg/mL rSe-HA for further 24 h. **(A)** MDA concentrations increased in OA-treated cells at 24 h, and those values remained unchanged at 48 h; similar results were observed in metformin-treated cells, whereas rSe-HA prevented MDA production. **(B)** Nitrite concentration was significantly increased in OA and metformin-treated cells, whereas rSe-HA reduced these levels. Data are reported as mean ± SD. The same letter in treatments or groups indicate that there are no significant differences between them; different letters in treatments indicate significant differences at $P < 0.05$. Differences with respect to untreated cells were analyzed by ANOVA and a Tukey-Kramer post hoc test. Significant differences with respect to the untreated group ($P \leq 0.001$) are indicated by different letters.

parameter was reduced by 120 % in metformin-treated cells. On the other hand, nitrite concentrations in rSe-HA-treated cells were similar to those in untreated control cells, with values 117.8 % lower than those induced by OA. These results indicate that rSe-HA controlled the prooxidant environment induced by OA.

3.7. rSe-HA reverses TNFα and IL6 content

Considering that several inflammatory markers are increased during hepatic steatosis, to ascertain whether rSe-HA controls the expression of proinflammatory cytokines such as TNFα and IL6—both related to a prooxidant state, IR, and lipid production—, the concentrations of both cytokines in the culture medium were measured by ELISA. HepG2 hepatocytes were cultured as described above, but these assays were focused on a decreased expression of TNFα and IL6. As shown in Fig. 6, no differences in the production of both cytokines were observed in untreated cells at 24 or 48 h. In contrast, an increase by 80 % and 86.3 % in TNFα (Fig. 6a) and IL6 levels (Fig. 6b), respectively, was observed in OA-treated cells at 24 h of culture. Additionally, the levels of IL6 were increased by 20 % in OA-stimulated cells at 48 h of culture with respect to 24 h values ($P < 0.001$). On the other hand, IL6 concentrations decreased by 82.1 % and 83.4 %, respectively, in metformin- and rSe-HA-treated cells, whereas those of TNFα were reduced by 91.3 % with metformin and 90.6 % with rSe-HA at 48 h of culture. This indicates that rSe-HA influences the production of cytokines that contribute to the proinflammatory status due to steatosis.

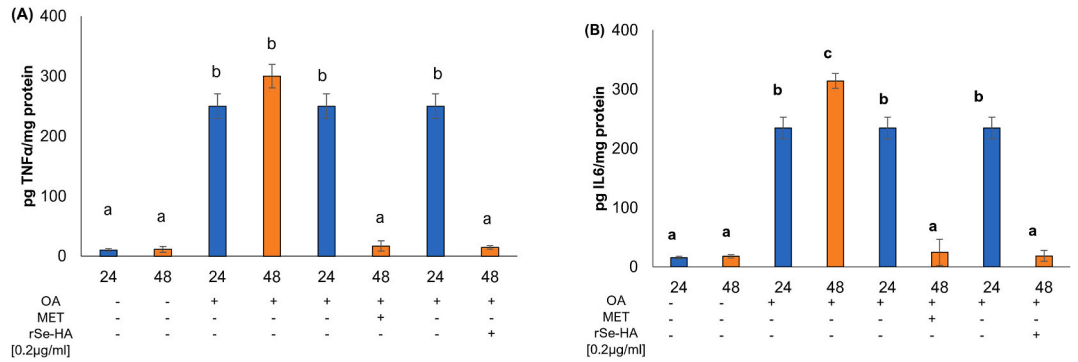

Fig. 6. CYTOKINE QUANTIFICATION. Effect of OA, metformin, and rSe-HA on TNFα and IL6 production by hepatocytes. **(A)** HepG2 cells were treated for 24 h with OA to induce steatosis, and another 24 h with OA plus either 2 mM metformin or 0.20 µg/mL rSe-HA. TNFα levels increased in OA-treated cells, while metformin and rSe-HA prevented this increase. **(B)** OA increased IL6 concentration, while metformin and rSe-HA reduced it. Data are reported as mean ± SD. The same letter in treatments or groups indicate that there are no significant differences between them; different letters in treatments indicate significant differences at $P < 0.05$. Differences with respect to untreated cells were analyzed by ANOVA and a Tukey-Kramer post hoc test. Significant differences with respect to the untreated group ($P \leq 0.001$) are indicated by different letters.

4. Discussion

In this work, we demonstrated the efficacy of a hydroalcoholic extract of the roots of *S. edule* (rSe-HA) to control the conditions that often accompany MAFLD, such as steatosis, insulin resistance, OS, and the production of proinflammatory cytokines [8,21] in HepG2 hepatic cells exposed to OA. MAFLD or NASH can be induced either by ANGII or OA; however, it should be highlighted that the development of both conditions is different. ANGII-induced MAFLD is mainly due to mitochondrial dysfunction and activation of lipogenic transcription factors, such as SREBP2 [27,28], whereas OA-induced MAFLD is mainly due to activation of transcription factors such as PPARγ and SREBP1c. Regardless of whether it is due to ANGII or OA, catabolic saturation of the cell and the establishment of a proinflammatory environment [3,4] is observed in all cases. Herein, the OA model was used to evaluate the effect of rSe-HA to decrease steatosis, OS, and proinflammatory cytokine production in dysfunctional HepG2 cells.

EC_{50} determination for rSe-HA was based on lipid accumulation in this OA-induced steatosis model. This concentration was indeed lower than that of metformin, suggesting that rSe-HA is more potent to revert lipid accumulation; this finding is reinforced by the E_{max} (0.7 μg/mL), a lower value than that of metformin (1.4 μg/mL) [29]. On the other hand, when comparing the EC_{50} calculated in this study with values reported by other authors who assayed the aerial parts of the plant *in vitro* [13] in the same model. It is noteworthy that the root extracts assayed in this study proved to be more potent; while effective concentrations of 1–5 mg/mL were reported by Wu et al. (2014) [13], our root extract was effective in levels as low as 0.20 μg/mL, one-fourth to one-fifth of the previously reported concentrations. These results support the therapeutic use of the root extract. Interestingly, commercial cinnamic acid was evaluated in the same model at concentrations of 25–200 μM [16]. In comparison, the EC_{50} of rSe-HA only contains 0.27 ng/mL of cinnamic acid, equivalent to 1.8×10^{-6} μM. This implies that the efficacy of rSe-HA may not solely be due to cinnamic acid (along with coumaric acid and some terpenes found in the extract), but to the interaction of its constituent molecules. Indeed, anti-lipogenic, anti-inflammatory, and antioxidant effects have been reported for both cinnamic and coumaric acid phenolic acids [30–34]. Although other compounds of terpenoid nature were also found in rSE-HA, no effects on the control of lipid metabolism have been reported for them. Nevertheless, some of those constituents are known to have antioxidant and inflammatory properties [35,36]. The fact that the extract is effective with such a low dose of cinnamic acid, even though it is its most abundant constituent, is a beneficial feature, as a prolonged consumption of cinnamic acid at high concentrations is toxic [37].

OA induces steatosis by deregulating lipid synthesis and degradation in the cell, inducing mitochondrial dysfunction [15]. This condition is related to a low activity of AMPK kinase and other enzymes downstream of catabolic processes [38,27]. Therefore, this kinase is an important therapeutic target for steatosis, as it has been observed for metformin [18]. Indeed, phosphorylated AMPK kinase activates lipases to degrade TGs, increasing glycerol concentration. It also activates mitochondrial enzymes to degrade lipids by β-oxidation, which is related to an increase in the reducing potential of the cell; on the other hand, it inhibits fatty acid synthase and diacylglycerol acyl transferase, preventing the formation of lipids and TG [21,23,24,39]. To gain further insight into the mode of action of the extract, its activity was compared with that of metformin, which is known to phosphorylate this enzyme at Thr^{172} [27,18,40]. Our results indicate that activation of AMPK at the Thr^{172} residue is one of the pathways by which the extract prevents intracellular TG accumulation (Fig. 3a), as does metformin (Fig. 3D, F). This activity has also been described for cinnamic and coumaric acid [12–16, 30,41], both found in rSe-HA. This effect is evidenced by the lower TG concentration and higher glycerol concentration in the cells. Both parameters are related to increased reducing power, suggesting that β-oxidation is also promoted (Fig. 3C). On the other hand, the continued presence of OA increased the concentration of AMPK in the cells, as the synthesis of this enzyme is promoted to reduce excess fat (Fig. 3 E). However, AMPK activation is not sufficient to degrade the excess of TG, as shown by the lower glycerol concentration and reducing power (Fig. 3A-C). This result is comparable to that reported by Lu et al. [15] who found that, after 48 h of treatment with OA alone, the cell shows mitochondrial dysfunction due to saturation of lipolytic enzymes.

While not evaluated in this work, it is feasible that the extract may also act at the level of fatty acids synthesis, since OA activates lipogenic transcription factors such as PPARγ and SREBP1c [42,43], which induce the expression of genes coding for enzymes involved in lipid esterification to TG [39]. Metformin acts by inhibiting the activation of these transcription factors, and a similar activity has been reported for cinnamic and coumaric acid [13,14,16,44].

TNFα and IL6 have been reported to mediate the induction of metabolic disorders [3,45,46], and both cytokines cause IR [3,45,46]. IR does not only reduce glucose consumption in the cell, but it also induces an uncontrolled activation of lipolysis, which increases intracellular ROS levels [46]. Thus, the efficacy of rSe-HA to overcome IR—as measured by glucose consumption—and to prevent TNFα and IL6 production was herein evaluated. Our results indicate that OA decreased glucose consumption by hepatocytes (Fig. 5), which is linked to an increased concentration of TNFα and IL6 in culture medium. This is consistent with reports by several authors that OA activates NFκB, so hepatocytes produce TNFα and IL6 [3,37,46]; in turn, these molecules induce IR by phosphorylating IRS1 at Ser^{312} [45,46]. This effect is reflected in a lower glucose consumption [46,47]. In our work, cells exposed to OA for 24 h showed lower intracellular glucose concentrations, which could be associated with IR, as well as a significantly higher production of TNFα and IL6. When treated with either rSe-HA or metformin for 24 h, even without interrupting the OA stimulus, hepatocytes were returned to the level of control cells; in fact, glucose consumption was even higher than in untreated cells. These results indicate an increased insulin sensitivity, as reflected by increased glucose consumption. Interestingly, the extract was able to reverse the phosphorylation of IR at Ser in a similar manner to metformin [48], as shown in Fig. 4. While not evaluated in this work, it is likely that rSe-HA not only offsets IR by reversing Ser phosphorylation, but it could also induce phosphorylation of IRS1 at Tyr, as it has been reported for metformin [48, 49]. On the other hand, rSe-HA could also prevent IR by reducing the production of proinflammatory cytokines [50–54], thus breaking the cycle of events. Cinnamic acid, coumaric acid, and squalene, all of which are present in the extract, have been reported to act similarly to metformin, favoring IRS phosphorylation at Tyr and preventing NFκB activation [50–54]. This beneficial effect of rSe-HA was also observed by our research group in *in-vivo* models, where rSe-HA reversed IR in diet-induced obese mice and reduced the

expression of TNFα and IL6 under the same conditions, as well as in models of NASH and endothelial dysfunction (ED) induced by ANGII [55,10,56].

OS plays a crucial role in the development of MAFLD and more severe diseases, such as NASH and cirrhosis [57]. MDA and nitrites are generated in OS due to ROS in fatty liver disease [58]. ROS oxidize polyunsaturated fatty acids in cell membranes, producing MDA [59], and activates iNOS, generating nitric oxide (NO), which in turn produces nitrites [25]. Both MDA and nitrites induce IR, inflammation, necrosis, and fibrosis [57]. ROS are originated from an overactivation of lipolysis by excess TG and fatty acids [57] and from the activity of OA, TNFα, and IL6, NADPH oxidase and iNOS in the hepatocyte [60,61]. Stopping and preventing ROS production is crucial to control the disease. In this study, the levels of MDA and nitrite (which indirectly promote a pro-oxidant environment) were significantly increased in hepatocytes exposed to OA for 48 h with respect to untreated cells; this result is consistent with other reports [58,59]. Metformin did not show antioxidant activity, as previously reported [7], while rSe-HA effectively decreased the concentration of MDA and nitrites to match the levels in control cells. This result highlights the usefulness of the extract over metformin, as the latter, while enhancing lipolysis, does not modify the pro-oxidative environment, whereas the extract not only increased lipolysis but also reduced the synthesis of molecules involved in OS. The antioxidant effect of the extract may be due to various molecules found to be present (including coumaric acid, cinnamic acid, methyl tetradecanoate, hexadecanoic acid, squalene, and stigmasterol), for which antioxidant properties have been reported, and may act as scavengers by interacting with unpaired electrons in ROS and by inducing the activation of Nrf2 through the PKC signaling pathway [32–35,61,62].

Strengths and limitations of the study. This study provides insight into some aspects of the mode of action of rSe-HA on hepatic steatosis. First, the extract not only decreased triglyceride levels, but it also prevented their synthesis, so it should be evaluated whether it inhibits the lipogenic transcription factors SREBP1c and PPARγ, whose inactivation prevents triglyceride synthesis. rSe-HA has also been reported to activate triglyceride degradation through AMPK kinase. However, it has yet to be determined whether, upon triglyceride cleavage, it also degrades the three free fatty acids into ketone bodies. Further studies should be performed to explore this possibility.

Interestingly, rSe-HA also overcame IR, as evidenced by a restored glucose uptake and low IRS phosphorylation at Ser^{312}; it also sensitized the cell to further glucose uptake, an effect similar to that of metformin. The latter could be either because it induces IRS phosphorylation at Tyr or because it activates AKT, which sensitizes the cell to insulin. This point remains to be clarified.

rSe-HA was efficient in decreasing the concentration of two molecules that contribute to the prooxidant environment (MDA and NO). To ascertain whether it induces the production of antioxidant enzymes, it would be convenient to evaluate the activation of Nrf2. Further studies are required to explore the effect of rSe-HA on ROS, such as the concentration of H_2O_2 and O^{2-}, as it also acts as a scavenger, so these parameters will provide further insight into the antioxidant effect.

Finally, rSe-HA reduces the concentration of the proinflammatory molecules TNFα and IL6, which could be due to its action on the transcription factor NFκB.

Taken together, these results point to the potential use of rSe-HA to treat fatty liver not only in patients with ED caused by ANGII, but also in patients with obesity and T2DM, reducing the individual use of conventional drugs such as antihyperglycemic, anti-inflammatory, antihypertensive and antioxidant drugs, and thus avoiding polypharmacy, since the extract fulfills all these actions even more potently than metformin, especially in the control of the prooxidative environment.

5. Conclusion

These results indicate that rSe-HA is effective in controlling intracellular TG accumulation. By increasing lipolysis, it prevents the production of cytokines like TNFα and IL6, as well as IR, with the additional benefit of acting as an antioxidant, preventing the damaging effect of oxidative stress.

Data availability

Data will be made available on request.

CRediT authorship contribution statement

Zimri Aziel Alvarado-Ojeda: Writing – original draft, Methodology, Investigation, Formal analysis, Conceptualization. **Alejandro Zamilpa:** Methodology, Formal analysis. **Alejandro Costet-Mejia:** Methodology. **Marisol Méndez-Martínez:** Methodology, Investigation. **Celeste Trejo-Moreno:** Methodology. **Jesús Enrique Jiménez-Ferrer:** Investigation. **Ana Maria Salazar-Martínez:** Methodology, Funding acquisition. **Mario Ernesto Cruz-Muñoz:** Methodology, Investigation. **Gladis Fragoso:** Writing – review & editing, Writing – original draft, Supervision, Investigation, Funding acquisition, Formal analysis. **Gabriela Rosas-Salgado:** Writing – original draft, Supervision, Investigation, Funding acquisition, Formal analysis, Conceptualization.

Declaration of competing interest

The authors declare the following financial interests/personal relationships which may be considered as potential competing interests:Gabriela Rosas-Salgado reports article publishing charges was provided by Consejo Nacional de Humanidades Ciencia y Tecnología. Gabriela Rosas-Salgado has patent COMPOSICIÓN FITOFARMACOLÓGICA DE EXTRACTO DE SECHIUM EDULE. licensed to TÍTULO DE PATENTE No. 377694. If there are other authors, they declare that they have no known competing financial interests or

personal relationships that could have appeared to influence the work reported in this paper.

Acknowledgments

The authors thank Juan Francisco Rodriguez for copyediting the original manuscript; thanks to, MCP. Miguel Angel Corona Alarcón, M.C Juan Carlos Villegas García. For their technical support. Marisol Mendez-Martinez thanks CONAHCyT for the post-doctoral fellowship (I1200-94-2020). Zimri Aziel Alvarado-Ojeda thanks CONAHCyT for the postgrad fellowship (1019271).

Abbreviations

MAFLD	Metabolic dysfunction associated fatty liver
HS	hepatic steatosis
NASH	nonalcoholic steatohepatitis
IR	insulin resistance
rSe-HA	*Sechium edule* root hydroalcoholic extract
ON	nitric oxide
ANGII	angiotensin II
OA	oleic acid
MS	metabolic syndrome
ALT/GPT	alanine amino transferase
OA/BSA	oleic acid-albumin
RT	room temperature
TG	triglyceride
MTT	3-(4,5-dimethylthiazol-2-yl)-2,5-diphenyltetrazole
MDA	malondialdehyde
TMB	tetramethylbenzidine
CA	cinnamic acid
ROS	reactive oxygen species
Non-Tx	non-treated
MET	metformin
ED	endothelial dysfunction

Appendix A. Supplementary data

Supplementary data to this article can be found online at https://doi.org/10.1016/j.heliyon.2024.e24567.

References

[1] T. Arshad, P. Golabi, L. Henry, Z.M. Younossi, Epidemiology of non-alcoholic fatty liver disease in North America, Curr. Pharmaceut. Des. 26 (2020) 993–997, https://doi.org/10.2174/1381612826666200303114934.
[2] R. Bernal-Reyes, G. Castro-Narro, R. Malé-Velázquez, R. Carmona-Sánchez, M.S. González-Huezo, I. García-Juárez, N. Chávez-Tapia, C. Aguilar-Salinas, I. Aiza-Haddad, M.A. Ballesteros-Amozurrutia, F. Bosques-Padilla, M. Castillo-Barradas, J.A. Chávez-Barrera, L. Cisneros-Garza, J. Flores-Calderón, D. García-Compeán, Y. Gutiérrez-Grobe, M.F. Higuera de la Tijera, D. Kershenobich-Stalnikowitz, L. Ladrón de Guevara-Cetina, J.A. Velarde-Ruiz Velasco, The Mexican consensus on nonalcoholic fatty liver disease, Rev. Gastroenterol. México 84 (2019) 69–99, https://doi.org/10.1016/j.rgmx.2018.11.007. English, Spanish.
[3] J.D. Browning, J.D. Horton, Molecular mediators of hepatic steatosis and liver injury, JCL 114 (2004) 147–152, https://doi.org/10.1172/JCI22422.
[4] F. Nassir, R.S. Rector, G.M. Hammoud, J.A. Ibdah, Pathogenesis and prevention of hepatic steatosis, GastroHep 11 (2015) 167–175.
[5] M. Sanjinez Asbún, C. Nishi, I. López Bilbao, G. Urquizo Ayala, Prevalencia de esteatosis hepática no alcohólica en pacientes diabéticos tipo 2, con o sin síndrome metabólico, Rev. Méd. La Paz 23 (2017) 12–17. La Paz.
[6] J.D. Browning, Statins and hepatic steatosis: perspectives from the Dallas Heart Study, Hepatology (Baltimore, Md 44 (2010) 466–471, https://doi.org/10.1002/hep.21248.
[7] R.A. DeFronzo, A.M. Goodman, Efficacy of metformin in patients with non-insulin-dependent diabetes mellitus. The Multicenter Metformin Study Group, NEJM 333 (1995) 541–549, https://doi.org/10.1056/NEJM199508313330902.
[8] S. Schuster, D. Cabrera, M. Arrese, A.E. Feldstein, Triggering and resolution of inflammation in NASH, Nature Rev. GastroHep. 15 (2018) 349–364, https://doi.org/10.1038/s41575-018-0009-6.
[9] T.S. Ferreira, C.Z. Moreira, N.Z. Cária, G. Victoriano, W.F. Silva Jr., J.C. Magalhães, Phytotherapy: an introduction to its history, use and application, Rev. Bras. Plantas Med. 16 (2014) 290–298, https://doi.org/10.1590/S1516-05722014000200019.
[10] A. Alvarado-Ojeda Zimri, A. Costet Mejia, G. Arrellin Rosas, J.E. Jiménez-Ferrer, A. Zamilpa, C. Trejo-Moreno, G. Castro Martínez, M. Méndez Martínez, J. Cervantes Torres, J.C. Báez Reyes, G. Fragoso, G. Rosas Salgado, Hepatoprotective effect of hydroalcoholic extract from root of *Sechium edule* (Jacq.) Sw. over hepatic injury induced by chronic application of ANGII, Front. Nat. Produc 1 (2022) 1–14, https://doi.org/10.3389/fntpr.2022.1043685.
[11] Trejo-Moreno, G. Castro-Martínez, M. Méndez-Martínez, J.E. Jiménez-Ferrer, J. Pedraza-Chaverri, G. Arrellín, A. Zamilpa, O.N. Medina-Campos, G. Lombardo-Earl, G.J. Barrita-Cruz, B. Hernández, C.C. Ramírez, M.A. Santana, G. Fragoso, G. Rosas, Acetone fraction from *Sechium edule* (Jacq.) S.w. edible roots exhibit anti-endothelial dysfunction activity, J. Ethnopharmacol. 220 (2018) 75–86, https://doi.org/10.1016/j.jep.2018.02.036.
[12] S.A. Yoon, S.I. Kang, H.S. Shin, S.W. Kang, J.H. Kim, H.C. Ko, S.J. Kim, p-Coumaric acid modulates glucose and lipid metabolism via AMP-activated protein kinase in L6 skeletal muscle cells, Biochem. Biophys. Res. Commun. 432 (2013) 553–557, https://doi.org/10.1016/j.bbrc.2013.02.067.

[13] C.H. Wu, T.T. Ou, C.H. Chang, X.Z. Chang, M.Y. Yang, C.J. Wang, The polyphenol extract from *Sechium edule* shoots inhibits lipogenesis and stimulates lipolysis via activation of AMPK signals in HepG2 cells, J. Agric. Food Chem. 62 (2014) 750–759, https://doi.org/10.1021/jf404611a.

[14] H. Nam, H. Jung, Y. Kim, B. Kim, K.H. Kim, S.J. Park, J.G. Suh, Aged black garlic extract regulates lipid metabolism by inhibiting lipogenesis and promoting lipolysis in mature 3T3-L1 adipocytes, Food Sci. Biotechnol. 27 (2017) 575–579, https://doi.org/10.1007/s10068-017-0268-y.

[15] Lu, J., Meng, Z., Cheng, B., Liu, M., Tao, S., Guan, S. Apigenin reduces the excessive accumulation of lipids induced by palmitic acid via the AMPK signaling pathway in HepG2 cells. Exp. Ther. Med.. https://doi.org/10.3892/etm.2019.7905.

[16] Y. Wu, M. Wang, T. Yang, L. Qin, Y. Hu, D. Zhao, L. Wu, T. Liu, Cinnamic acid ameliorates nonalcoholic fatty liver disease by suppressing hepatic lipogenesis and promoting fatty acid oxidation, Evid. Based Complement Alternat. Med 9561613 (2021), https://doi.org/10.1155/2021/9561613.

[17] J. Araya, R. Rodrigo, L.A. Videla, L. Thielemann, M. Orellana, P. Pettinelli, J. Poniachik, Increase in long-chain polyunsaturated fatty acid n - 6/n - 3 ratio in relation to hepatic steatosis in patients with non-alcoholic fatty liver disease, Clin. Sci. (Lond.) 106 (2004) 635–643, https://doi.org/10.1042/CS20030326.

[18] X. Zhu, H. Yan, M. Xia, X. Chang, X. Xu, L. Wang, X. Sun, Y. Lu, H. Bian, X. Li, X. Gao, Metformin attenuates triglyceride accumulation in HepG2 cells through decreasing stearyl-coenzyme A desaturase 1 expression, Lipids Health Dis. 17 (2018) 114. http://doi:10.1186/s12944-018-0762-0.

[19] The Plant List, A working list of all plant species. http://www.theplantlist.org, 2013.

[20] O. Alarcón Corredor, M.R. de Fernández, E. Carnevalí de Tatá, Los mapas enzimáticos tisulares y séricos y la utilidad diagnóstica de los cocientes enzimáticos: una revisión, MedULA 7 (1998) 19–24. http://www.saber.ula.ve/handle/123456789/21677.

[21] W. Cui, S.L. Chen, K.Q. Hu, Quantification and mechanisms of oleic acid-induced steatosis in HepG2 cells, Am J Transl Res 2 (2010) 95–104.

[22] M.M. Marisol, T.M. Celeste, M.M. Laura, E.G. Fernando, P.C. José, Z. Alejandro, M.C. Omar, A.A. Francisco, A.P. Julio César, C.N. Erika, S.C. Angélica, F. Gladis, J.F. Enrique, R. Gabriela, Effect of *Cucumis sativus* on dysfunctional 3T3-L1 adipocytes, Sci. Rep. 9 (2019) 13372, https://doi.org/10.1038/s41598-019-49458-6.

[23] R.L. Veech, The therapeutic implications of ketone bodies: the effects of ketone bodies in pathological conditions: ketosis, ketogenic diet, redox states, insulin resistance, and mitochondrial metabolism, Prostaglandins Leukot. Essent. Fatty Acids 70 (2004) 309–319, https://doi.org/10.1016/j.plefa.2003.09.007.

[24] Y. Rai, R. Pathak, N. Kumari, D.K. Sah, S. Pandey, N. Kalra, R. Soni, B.S. Dwarakanath, A.N. Bhatt, Mitochondrial biogenesis and metabolic hyperactivation limits the application of MTT assay in the estimation of radiation induced growth inhibition, Sci. Rep. 8 (2018) 1531, https://doi.org/10.1038/s41598-018-19930-w.

[25] K.M. Miranda, M.G. Espey, D.A. Wink, A rapid, simple spectrophotometric method for simultaneous detection of nitrate and nitrite, Nitric Oxide 5 (2001) 62–71, https://doi.org/10.1006/niox.2000.0319.

[26] S. Spahis, E. Delvin, J.-M. Borys, E. Levy, Oxidative stress as a critical factor in nonalcoholic fatty liver disease pathogenesis, Antioxidants Redox Signal. 26 (2017) 519–541, https://doi.org/10.1089/ars.2016.6776.

[27] Y. Wu, K.L. Ma, Y. Zhang, Y. Wen, G.H. Wang, Z.B. Hu, L. Liu, J. Lu, P.P. Chen, X.Z. Ruan, B.C. Liu, Lipid disorder and intrahepatic renin–angiotensin system activation synergistically contribute to non-alcoholic fatty liver disease, Liver Int. 36 (2016) 1525–1534, https://doi.org/10.1111/liv.13131.

[28] Y. Wei, S.E. Clark, E.M. Morris, J.P. Thyfault, G.M. Uptergrove, A.T. Whaley-Connell, C.M. Ferrario, J.R. Sowers, J.A. Ibdah, Angiotensin II-induced non-alcoholic fatty liver disease is mediated by oxidative stress in transgenic TG (mRen2)27(Ren2) rats, J. Hepatol. 49 (2008) 417–428, https://doi.org/10.1016/j.jhep.2008.03.018.

[29] C. Di Verniero, C. Höcht, J.A. Opezzo, C.A. Taira, Propiedades farmacodinámicas in vitro de los bloqueantes a-adrenérgicos propranolol y atenolol en ratas con coartación aórtica, Rev. Argent. Cardiol. 71 (2003) 339–343.

[30] Y. Wu, M. Wang, T. Yang, L. Qin, Y. Hu, D. Zhao, L. Wu, T. Liu, Cinnamic acid ameliorates nonalcoholic fatty liver disease by suppressing hepatic lipogenesis and promoting fatty acid oxidation, Evid. Based Complement Alternat. Med 2021 (2021) 9561613, https://doi.org/10.1155/2021/9561613.

[31] X. Yan, X. Chen, X. Xu, J. Liu, C. Fu, D. Zhao, W. Zhao, R. Ma, L. Sun, Mechanism underlying p-coumaric acid alleviation of lipid accumulation in palmitic acid-treated human hepatoma cells, J. Agric. Food Chem. 68 (12) (2020) 3742–3749, https://doi.org/10.1021/acs.jafc.0c00280.

[32] S.J. Pragasam, V. Venkatesan, M. Rasool, Immunomodulatory and anti-inflammatory effect of p-coumaric acid, a common dietary polyphenol on experimental inflammation in rats, Inflammation 36 (1) (2013) 169–176, https://doi.org/10.1007/s10753-012-9532-8.

[33] D. Hadjipavlou-Litina, E. Pontiki, Aryl-acetic and cinnamic acids as lipoxygenase inhibitors with antioxidant, anti-inflammatory, and anticancer activity, Methods Mol. Biol. 1208 (2015) 361–377, https://doi.org/10.1007/978-1-4939-1441-8_26.

[34] Y. Shen, X. Song, L. Li, J. Sun, Y. Jaiswal, J. Huang, C. Liu, W. Yang, L. Williams, H. Zhang, Y. Guan, Protective effects of p-coumaric acid against oxidant and hyperlipidemia-an in vitro and in vivo evaluation, Biomed. Pharmacother. 111 (2019) 579–587, https://doi.org/10.1016/j.biopha.2018.12.074.

[35] A. Cárdeno, M. Aparicio-Soto, S. Montserrat-de la Paz, B. Bermúdez, F.J. Muriana, C. Alarcón-de-la-Lastra, Squalene targets pro-and anti-inflammatory mediators and pathways to modulate over-activation of neutrophils, monocytes and macrophages, J. Funct.Foods 14 (2015) 779–790.

[36] C.I.B. Walker, S.M. Oliveira, R. Tonello, M.F. Rossato, E. da Silva Brum, J. Ferreira, G. Trevisan, Anti-nociceptive effect of stigmasterol in mouse models of acute and chronic pain, Naunyn-Schmiedeberg's Arch. Pharmacol. 390 (11) (2017) 1163–1172, https://doi.org/10.1007/s00210-017-1416-x.

[37] J.A. Hoskins, The occurrence, metabolism, and toxicity of cinnamic acid and related compounds, J. Appl. Toxicol. 4 (1984) 283–292, https://doi.org/10.1002/jat.2550040602.

[38] Y. Wei, S.E. Clark, J.P. Thyfault, G.M. Uptergrove, W. Li, A.T. Whaley-Connell, C.M. Ferrario, J.R. Sowers, J.A. Ibdah, Oxidative stress-mediated mitochondrial dysfunction contributes to angiotensin II-induced nonalcoholic fatty liver disease in transgenic Ren2 rats, Am. J. Pathol. 174 (2009) 1329–1337, https://doi.org/10.2353/ajpath.2009.080697.

[39] S.H. Koo, Nonalcoholic fatty liver disease: Molecular mechanisms for the hepatic steatosis, Clin. Mol. Hepatol. 19 (2013) 210–215. https://doi:10.3350/cmh.2013.19.3.210.

[40] Y. Jiang, W. Huang, J. Wang, Z. Xu, J. He, X. Lin, Z. Zhou, J. Zhang, Metformin plays a dual role in MIN6 pancreatic β cell function through AMPK-dependent autophagy, Int. J. Biol. Sci. 10 (2014) 268–277, https://doi.org/10.7150/ijbs.7929.

[41] C. Kopp, S.P. Singh, P. Regenhard, U. Müller, H. Sauerwein, M. Mielenz, Trans-cinnamic acid increases adiponectin and the phosphorylation of AMP-activated protein kinase through G-protein-coupled receptor signaling in 3T3-L1 adipocytes, Int. J. Mol. Sci. 15 (2) (2014) 2906–2915, https://doi.org/10.3390/ijms15022906.

[42] M. Ricchi, M.R. Odoardi, L. Carulli, C. Anzivino, S. Ballestri, A. Pinetti, L.I. Fantoni, F. Marra, M. Bertolotti, S. Banni, A. Lonardo, N. Carulli, P. Loria, Differential effect of oleic and palmitic acid on lipid accumulation and apoptosis in cultured hepatocytes, J. Gastroenterol. Hepatol. 24 (2009) 830–840, https://doi.org/10.1111/j.1440-1746.2008.05733.x.

[43] A.C. Poletto, D.T. Furuya, A. David-Silva, P. Ebersbach-Silva, M.L. Corrêa -Giannella, M. Passarelli, U.F. Machado, Oleic and linoleic fatty acids downregulate Slc2a4/GLUT4 expression via NFKB and SREBP1 in skeletal muscle cells, Mol. Cell. Endocrinol. 401 (2015) 65–72, https://doi.org/10.1016/j.mce.2014.12.001.

[44] L. Zhao, S.J. Jiang, F.E. Lu, L.J. Xu, X. Zou, K.F. Wang, H. Dong, Effects of berberine and cinnamic acid on palmitic acid-induced intracellular triglyceride accumulation in NIT-1 pancreatic β cells, Chin. J. Integr. Med. 22 (2016) 496–502, https://doi.org/10.1007/s11655-014-1986-0.

[45] K. Tokushige, E. Hashimoto, N. Tsuchiya, H. Kaneda, M. Taniai, K. Shiratori, Clinical significance of soluble TNF receptor in Japanese patients with non-alcoholic steatohepatitis, Alcohol Clin. Exp. Res. 29 (SUPPL) (2005) 298–303, https://doi.org/10.1097/01.alc.0000191810.46000.37.

[46] S.R. Nagarajan, M. Paul-Heng, J.R. Krycer, D.J. Fazakerley, A.F. Sharland, A.J. Hoy, Lipid and glucose metabolism in hepatocyte cell lines and primary mouse hepatocytes: a comprehensive resource for in vitro studies of hepatic metabolism, Am. J. Physiol. Endocrinol. Metab. 316 (2019) E578–E589, https://doi.org/10.1152/ajpendo.00365.2018.

[47] C. Batandier, B. Guigas, D. De taille, M.Y. El-Mir, E. Fontaine, M. Rigoulet, X.M. Leverve, The ROS production induced by a reverse-electron flux at respiratory-chain complex 1 is hampered by metformin, J. Bioenerg. Biomembr. 38 (2006) 33–42, https://doi.org/10.1007/s10863-006-9003-8.

[48] W. Wu, S. Tang, J. Shi, W. Yin, S. Cao, R. Bu, D. Zhu, Y. Bi, Metformin attenuates palmitic acid-induced insulin resistance in L6 cells through the AMP-activated protein kinase/sterol regulatory element-binding protein-1c pathway, Int. J. Mol. Med. 35 (2015) 1734–1740, https://doi.org/10.3892/ijmm.2015.2187.

[49] J. Deng, M. Peng, S. Zhou, D. Xiao, X. Hu, S. Xu, J. Wu, X. Yang, Metformin targets Clusterin to control lipogenesis and inhibit the growth of bladder cancer cells through SREBP-1c/FASN axis, Signal Transduct. Targeted Ther. 6 (2021) 98, https://doi.org/10.1038/s41392-021-00493-8.

[50] C. Nicholas, S. Batra, M.A. Vargo, O.H. Voss, M.A. Gavrilin, M.D. Wewers, D.C. Guttridge, E. Grotewold, A.I. Doseff, Apigenin blocks lipopolysaccharide-induced lethality in vivo and proinflammatory cytokines expression by inactivating NF-kB through the suppression of p65 phosphorylation, J. Immunol. 179 (2007) 7121–7127, https://doi.org/10.4049/jimmunol.179.10.7121.
[51] B. de las Heras, B. Rodríguez, L. Boscá, A.M. Villar, Terpenoids: sources, structure elucidation and therapeutic potential in inflammation, Curr. Top. Med. Chem. 3 (2003) 171–185, https://doi.org/10.2174/1568026033392462.
[52] X. Li, Z. Wen, X. He, S. He, Effects of cinnamic acid on expression of tissue factor induced by TNFalpha in endothelial cells and its mechanisms, J. Chin. Med. Assoc. 207–212 (2006), https://doi.org/10.1016/S1726-4901(09)70220-5.
[53] M.K. Neog, S. Joshua Pragasam, M. Krishnan, M. Rasool, p-Coumaric acid, a dietary polyphenol ameliorates inflammation and curtails cartilage and bone erosion in the rheumatoid arthritis rat model, Biofactors 43 (2017) 698–717, https://doi.org/10.1002/biof.1377.
[54] Hernández Acosta Julieta, Evaluación del efecto de la fracción acetónica de la raíz de *Sechium edule* sobre el daño cognitivo asociado a hipocampo en ratones con síndrome metabólico, in: Tesis de licenciatura en Biología, Universidad Autónoma del Estado de Morelos (UAEM), 2019.
[55] C. Trejo-Moreno, E. Jiménez-Ferrer, G. Castro-Martínez, M. Méndez-Martínez, M.A. Santana, G. Arrellín-Rosas, J. Pedraza-Chaverri, O.N. Medina-Campos, B. Hernández-Téllez, O. Ramírez-Pliego, M. Herrera-Ruiz, J. Cervantes-Torres, Z.A. Alvarado-Ojeda, A. Costet-Mejía, G. Fragoso, G. Rosas-Salgado, Characterization of a murine model of endothelial dysfunction induced by chronic intraperitoneal administration of angiotensin II, Sci. Rep. 11 (2021) 21193, https://doi.org/10.1038/s41598-021-00676-x.
[56] A. Elshamy, G. Omran, M. Abd-Alhaseeb, M. Houssen, Chemotherapeutic effect of stigmasterol in sorafenib treated breast cancer cell lines via modulation of NF-κB and ERK signaling pathways, Egypt, J. Chem. 67 (2024) 227–234, https://doi.org/10.21608/ejchem.2023.204388.7825.
[57] Z. Chen, R. Tian, Z. She, J. Cai, H. Li, Role of oxidative stress in the pathogenesis of nonalcoholic fatty liver disease, Free Radic. Biol. Med. 152 (2020) 116–141, https://doi.org/10.1016/j.freeradbiomed.2020.02.025.
[58] J. Zhang, S.D. Zhang, P. Wang, N. Guo, W. Wang, L.P. Yao, Q. Yang, T. Efferth, J. Jiao, Y.J. Fu, Pinolenic acid ameliorates oleic acid-induced lipogenesis and oxidative stress via AMPK/SIRT1 signaling pathway in HepG2 cells, Eur. J. Pharmacol. 861 (2019) 172618, https://doi.org/10.1016/j.ejphar.2019.172618.
[59] E. Hatanaka, A. Dermargos, A.E. Hirata, M.A. Vinolo, A.R. Carpinelli, P. Newsholme, H.A. Armelin, R. Curi, Oleic, linoleic and linolenic acids increase ROS production by fibroblasts via NADPH oxidase activation, PLoS One 8 (2013) e58626, https://doi.org/10.1371/journal.pone.0058626.
[60] Huiyong Yin, L. Xu, N.A. Porter, Free radical lipid peroxidation: mechanisms and analysis, Chem. Rev. 111 (2011) 5944–5972, https://doi.org/10.1021/cr200084z.
[61] H.E. de Vries, M. Witte, D. Hondius, A.J. Rozemuller, B. Drukarch, J. Hoozemans, J. van Horssen, Nrf2-induced antioxidant protection: a promising target to counteract ROS-mediated damage in neurodegenerative disease? Free Radic. Biol. Med. 45 (2008) 1375–1383, https://doi.org/10.1016/j.freeradbiomed.2008.09.001.
[62] Y.C. Hseu, M. Korivi, F.Y. Lin, M.L. Li, R.W. Lin, J.J. Wu, H.L. Yang, Trans-cinnamic acid attenuates UVA-induced photoaging through inhibition of AP-1 activation and induction of Nrf2-mediated antioxidant genes in human skin fibroblasts, J. Dermatol. Sci. 90 (2018) 123–134, https://doi.org/10.1016/j.jdermsci.2018.01.004.